JOURNAL OF GUIDANCE, CONTROL, AND DYNAMICS
Vol. 20, No. 4, July–August 1997

Maneuvering Flight Control with Actuator Constraints

R. B. Miller* and M. Pachter†
U.S. Air Force Institute of Technology, Wright–Patterson Air Force Base, Ohio 45433-7765

Tracking control is addressed. A receding horizon control framework is considered and a novel, optimization-based, linear tracking control strategy, linear quadratic tracking (LQT), is devised. LQT is used to obtain a closed-form solution to optimization-based tracking of a dynamic reference signal $r(t)$, in the face of both rate and amplitude actuator constraints. Actuator dynamics are considered. Also, there is no inherent requirement for stability of the open-loop plant. At the same time, full state feedback is assumed. The detrimental effects of the actuator constraints are mitigated by giving the control system a nonlinearly modified, feasible reference signal $r'(t)$, as required to prevent downstream actuator saturations from occurring. Thus, the controller generated signal never infringes on the saturation bounds, and saturation caused windup is avoided. The analytic solution to the linear, unconstrained, tracking problem meets the small signal performance specifications and is stable. The proposed piecewise linear closed-form solution to the constrained tracking problem yields satisfactory responses to large inputs and at the same time requires modest on-line computation, and hence, it is implementable in real time.

I. Introduction

ACTUATOR saturation is a topic of active research in control theory.[1–22] The current literature can be classified as follows. Most of the work is geared toward the regulation and set-point control problems as opposed to tracking control and, thus, does not directly apply to maneuvering and manual flight control. Also, most of the work fails to address actuator rate saturation. Notable exceptions, concerning tracking control are found in Refs. 4, 5, 10, 17, and 18, and rate saturation is considered in Refs. 4, 5, 7, 14, 17, and 18. In the tradition of Popov's work,[19] most papers are restricted to stable open-loop plants. Unstable plants are specifically addressed in Refs. 2, 4, 5, 7, 11–13, 17, 18, and 21. Additionally, by neglecting actuator dynamics altogether, actuator constraints are most often treated as control constraints, whereas, particularly in high-gain flight control, actuator dynamics should be included, in which case actuator constraints introduce state constraints into the control problem.

When an exogenous reference signal is being considered in the literature, the concept of tracking a less aggressive reference as a means of avoiding saturation has been proposed (e.g., Refs. 4, 5, 7, 10, 14, 15, 17, 18, and 21). Thus, the reference governor concept is advanced in Ref. 7. The original continuous-time developments are computationally complex, whereas in the discrete-time formulation in Ref. 7, the on-line solution of a sequence of linear programming problems is required. In the present paper, a novel, closed-form optimization-based approach is developed that is grounded in tracking control and, thus, allows for the tracking of a less aggressive pilot input reference signal.

Specifically, this paper addresses the actuator saturation problem (both amplitude and rate) from a manual flight control perspective and, hence, tracking control is considered. The approach acknowledges the existence of hard constraints from the outset. Actuator dynamics are included. There is no requirement for stability of the open-loop plant. At the same time, full state feedback is assumed. The exogenous system input is the reference signal from the pilot. The concept of tracking a less aggressive reference as a means of avoiding saturation is employed. An optimization-based, nonlinear, but closed-form feedback control strategy for the actuator constrained tracking problem is proposed.

The paper is organized as follows. The manual flight control problem is stated in Sec. II. The tracking control problem in state space and employing state feedback is concisely posed, and the term linear quadratic tracking (LQT) is coined. The proposed model-based receding horizon tracking control strategy is developed in Sec. III. The extrapolation of the reference signal and the attendant behavioral assumptions are discussed in Sec. IV. The unconstrained LQT problem is solved in Sec. V, and the treatment of hard control constraints is undertaken in Sec. VI. The control algorithm is obtained in a closed form yielding a computationally inexpensive and real-time implementable, fixed gain, state feedback control law and a readily determined nonlinear (up or down) scaling of the reference signal that prevents attempted violations of the downstream actuator constraints. The control law is piecewise linear, small signal stability and performance of the feedback control system is guaranteed, and good responses to large inputs are obtained. A flight control implementation and simulation results are presented in Sec. VII. Concluding remarks are made in Sec. VIII.

II. Manual Flight Control

Manual (and maneuvering) flight control plays a central role in military aviation, where the objective is to engage enemy aircraft or to attack ground targets. Thus, manual flight control calls for tracking control. The tracking problem begins at some point subsequent to takeoff and cruise (where the aircraft could be flown by the autopilot) and ends when the mission is completed. Thus, the manual tracking task is an open-ended problem, which evolves in time; its duration is unknown prior to the completion of the task.

Moreover, and particularly in the case of aircraft manual flight control, the tracking situation arises where the reference signal is not known in advance. Furthermore, these control problems are strictly of a dynamic and transient nature. This input variability contrasts the classical regulation paradigm. These considerations, and bearing in mind the very nature of hard actuator constraints, indicate that the manual flight control problem should be addressed in the time domain.

The constrained actuator control problem is most commonly treated as a control constrained problem, when, in fact, it is a state constrained problem. Consider the block diagram of Fig. 1, which represents the tracking feedback control problem at hand. The physical aircraft includes control surfaces that are positioned by dynamic actuators. The controller's output is $u \equiv \delta_c$, which, when linear controllers are employed, in general, is unconstrained. The control surface deflection δ, which is the plant's input, however, is constrained due to physical limitations of the mechanical actuator. In addition, an appropriate aircraft model requires an augmentation of the airframe dynamics with the actuator dynamics.

The basic airframe dynamics (plant) are described by

$$\boldsymbol{x}_{p_{k+1}} = \boldsymbol{A}_p \boldsymbol{x}_{p_k} + \boldsymbol{b}_p \delta_k + \boldsymbol{\zeta} d, \qquad k = 0, 1, \ldots, N-1 \qquad (1)$$

Received Oct. 1, 1996; revision received April 1, 1997; accepted for publication April 1, 1997.

*Ph.D. Student, Department of Electrical and Computer Engineering. E-mail: rbmiller@afit.af.mil.

†Professor, Department of Electrical and Computer Engineering. E-mail: mpachter@afit.af.mil. Member AIAA.

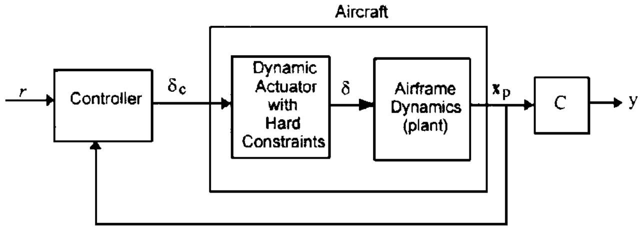

Fig. 1 Tracking problem block diagram.

where $\boldsymbol{x}_{p_k}$ is the plant state vector at time k, $\boldsymbol{A}_p$ and $\boldsymbol{b}_p$ are the dynamics matrix and input vector, respectively, δ_k is the control surface deflection at time k, $\boldsymbol{\zeta}$ is a disturbance input vector, d is a known and constant disturbance, and the output of interest is $y_{k+1} = \boldsymbol{c}_p \boldsymbol{x}_{p_{k+1}}$. N is the planning/optimization horizon. The inclusion of the known constant disturbance d is motivated by the need to linearize the plant about a nontrim point. $\boldsymbol{A}_p$ is not necessarily Hurwitz. Furthermore, the control surface displacement is constrained in both amplitude and rate, viz.,

$$\delta_{\min} \leq \delta_{k+1} \leq \delta_{\max} \tag{2}$$

$$\Delta\,\delta_{\min} \leq (\delta_{k+1} - \delta_k) \leq \Delta\,\delta_{\max}, \qquad k = 0, 1, \ldots, N-1 \tag{3}$$

The control system supplies actuator commands (the control signal, $u_k \equiv \delta_{c_k}$), resulting in control surface deflections according to the actuator dynamics, viz., $\boldsymbol{x}_{\delta_{k+1}} = \boldsymbol{A}_\delta \boldsymbol{x}_{\delta_k} + \boldsymbol{b}_\delta \delta_{c_k}$ and $\delta_{k+1} = \boldsymbol{c}_\delta \boldsymbol{x}_{\delta_{k+1}}$. The internal state of the actuator at time k is $\boldsymbol{x}_{\delta_k}$.

Thus, the flight control system under consideration entails an augmentation of the airframe dynamics. An integrator state z for the purpose of implementing integral action in the time domain is also included and adds a pole at the (s-plane) origin. The latter may be necessary in order to meet tracking performance specifications and/or the rejection of unmodeled disturbances. Hence, the augmented control system ensues:

$$\boldsymbol{x}_{k+1} \equiv \begin{bmatrix} \boldsymbol{x}_{p_{k+1}} \\ \hline \boldsymbol{x}_{\delta_{k+1}} \\ \hline z_{k+1} \end{bmatrix} = \left[\begin{array}{c|c|c} \boldsymbol{A}_p & \boldsymbol{b}_p \boldsymbol{c}_\delta & \boldsymbol{0} \\ \hline \boldsymbol{0} & \boldsymbol{A}_\delta & \boldsymbol{0} \\ \hline -T\boldsymbol{c}_p \boldsymbol{A}_p & \boldsymbol{0} & 1 \end{array}\right] \begin{bmatrix} \boldsymbol{x}_{p_k} \\ \hline \boldsymbol{x}_{\delta_k} \\ \hline z_k \end{bmatrix}$$

$$+ \begin{bmatrix} \boldsymbol{0} \\ \hline \boldsymbol{b}_\delta \\ \hline 0 \end{bmatrix} \delta_{c_k} + \begin{bmatrix} \boldsymbol{0} \\ \hline \boldsymbol{0} \\ \hline T \end{bmatrix} r_{k+1} + \begin{bmatrix} \zeta \\ \hline \boldsymbol{0} \\ \hline 0 \end{bmatrix} d \tag{4}$$

$$\boldsymbol{x}_{k+1} \equiv \boldsymbol{A}\boldsymbol{x}_k + \boldsymbol{b}u_k + \boldsymbol{\Gamma}_1 r_{k+1} + \boldsymbol{\Gamma}_2 d \tag{5}$$

$$y_{k+1} = [\boldsymbol{c}_p \mid \boldsymbol{0} \mid 0]\boldsymbol{x}_{k+1} \equiv \boldsymbol{c}\boldsymbol{x}_{k+1} \tag{6}$$

where the respective augmented state, input vector, output vector, and disturbance input vector are $\boldsymbol{x}_k, \boldsymbol{b}, \boldsymbol{c}^T, \boldsymbol{\Gamma}_2 \in \boldsymbol{R}^n$; the augmented dynamics matrix $\boldsymbol{A} \in \boldsymbol{R}^{n\times n}$; the control signal, the output, and the (constant and known) disturbance are $u_k, y_{k+1}, d, \in \boldsymbol{R}^1$, respectively; the time variable is $k = 0, 1, 2, \ldots, N-1$; and the initial state $\boldsymbol{x}_0 \in \boldsymbol{R}^n$ is known. Note that in the augmented system the additional input vector $\boldsymbol{\Gamma}_1 \in \boldsymbol{R}^n$ is needed to accommodate the inclusion of integral control, and T is the sampling interval. An examination of Eqs. (2–5) readily reveals that a constrained state problem is obtained.

III. Tracking Control

In Refs. 4, 5, 17, and 18, it has been recognized that a receding horizon predictive control (RHPC) approach is well suited to the tracking control problem and thus applicable to manual flight control. In these works the linear quadratic (LQ) and linear programming (LP) optimization paradigms have been combined to yield a hybrid approach to the control-constrained tracking problem within the RHPC framework. The LQ/LP approach to tracking ensures that for some time into the future only feasible signals are generated by the controller, which do not exceed the prescribed control constraints. A discrete-time formulation is employed. The present paper builds on those previous works, to yield a one-step ahead constraint enforcement scheme, which is readily implementable in closed form. Thus, the need for complex on-line numerical optimization is eliminated, and real-time operation is facilitated. Additionally, the actuator amplitude constraints are properly incorporated as state constraints, and the actuator rate constraints are properly incorporated as control and state constraints. Also, special attention is given to the reference signal extrapolation and the selection of the planning horizon.

The tracking task requires the system output to follow an exogenous reference, i.e., it is required that $y_{m+1} \approx r_{m+1}$, $m = k, k+1, \ldots, k+N-1$, and without too much control effort. In other words, the quadratic performance functional of the general form

$$J = \sum_{m=k}^{k+N-1} \left[Q_P(y_{m+1} - r_{m+1})^2 + Q_I z_{m+1}^2 + R u_m^2\right] \tag{7}$$

is to be minimized, where the scalar weights $Q > 0$ and $R > 0$. In tracking control, the reference signal r_{m+1} needs to be known for all $m = k, k+1, \ldots, k+N-1$, at time t_k.

As already discussed, in the manual tracking problem, it is required to continually follow an unknown, exogenous reference as it becomes available in time. Thus, r_{k+1} is not known until time k, at which time $r_{k+2}, \ldots, r_{k+N}$ are not known. Hence, at time k it is impossible to explicitly evaluate (or much less minimize) the performance functional J given in Eq. (7) for a given tracking task until it is over; clearly, at this point it is too late to utilize this information in the control of the vehicle during the tracking task. Thus, to employ the optimal control method, the reference signal r_k must be prespecified over the planning horizon. Inasmuch as this is not feasible in the case of manual, viz., real-time, tracking control at time k, the reference must be predicted into the future based on the currently available reference signal r_{k+1} and the past history of the reference signal.

Polynomial extrapolation is used. It would be ill advised to make long-term predictions, and so a receding horizon approach makes sense and is used to break up the infinite horizon tracking problem into an open-ended sequence of finite horizon optimization problems based on short-term only predictions of the reference. The choice of the optimization horizon N also requires further elaboration.

At each time instant k, i.e., within each RHPC window, the reference signal is extrapolated over the planning horizon N, within which the single-input unconstrained LQ tracking problem is posed as an optimization problem in $(u_k, u_{k+1}, \ldots, u_{k+N-1})^T \in \boldsymbol{R}^N$. The predicted reference signal is denoted by $\hat{r}_{k+n}$, $n = 2, \ldots, N$. Thus, over the duration of the optimization window, the reference signal is $(r_{k+1}, \hat{r}_{k+2}, \ldots, \hat{r}_{k+N})^T$. Hence, at each time step k, the (unconstrained) optimal control sequence $\boldsymbol{u}^* = (u_0^*, u_1^*, \ldots, u_{N-1}^*)^T$ for tracking the extrapolated reference sequence $\hat{\boldsymbol{r}} = (r_1, \hat{r}_2, \ldots, \hat{r}_N)^T$ is determined, such that the quadratic performance functional

$$J = \sum_{n=0}^{N-1} \left[Q_P(y_{n+1} - \hat{r}_{n+1})^2 + Q_I z_{n+1}^2 + R u_n^2\right] \tag{8}$$

is minimized. In the sequel, the subscript k will be used to represent real-time instants, whereas within a given receding horizon window, the subscript n will be used. Thus, each u_k and r_{k+1} over the tracking task will be represented by a u_0 and r_1, respectively, in one of the receding horizon windows.

According to the receding horizon method, u_0 represents an actual system input. The remaining control signals $u_1, \ldots, u_{N-1}$ do not represent physically realized inputs to the system. Furthermore, at any given time instant k in the system time reference, $\boldsymbol{x}_0$ from the window time reference represents $\boldsymbol{x}_k$; thus, state feedback action is achieved via the receding horizon formulation.

Now, with the reference signal r_k stipulated for all $l \leq k \leq N$, the unconstrained LQT problem with finite planning horizon N can be posed as an LQ optimization problem in the control sequence $(u_0, u_1, \ldots, u_{N-1})^T \in \boldsymbol{R}^N$ by considering the vectors

$$\boldsymbol{u} = [u_n] = (u_0, u_1, \ldots, u_{N-1})^T \in \boldsymbol{R}^N \tag{9}$$

$$\hat{\boldsymbol{r}} = [\hat{r}_n] = (r_1, \hat{r}_2, \ldots, \hat{r}_N)^T \in \boldsymbol{R}^N \tag{10}$$

$$\boldsymbol{y} = [y_n] = (y_1, y_2, \ldots, y_N)^T \in \boldsymbol{R}^N \tag{11}$$

$$\boldsymbol{z} = [z_n] = (z_1, z_2, \ldots, z_N)^T \in \boldsymbol{R}^N \tag{12}$$

where $\boldsymbol{u}$ represents an N-point input sequence, $\hat{\boldsymbol{r}}$ is the extrapolated reference sequence, $\boldsymbol{y}$ is the corresponding N-point output sequence, and z is the N-point integrator charge. Recall that the second through Nth components of $\boldsymbol{u}$ are never actually used to drive the system and, in fact, these components of $\boldsymbol{u}$ do not necessarily have to be explicitly computed. Additionally, the second through Nth elements of the output $\boldsymbol{y}$ are not actually realized.

Using the vector notation in Eqs. (9–12), the cost functional J is given by $J = Q_P[\boldsymbol{y} - \hat{\boldsymbol{r}}]^T[\boldsymbol{y} - \hat{\boldsymbol{r}}] + Q_I z^T z + R\boldsymbol{u}^T\boldsymbol{u}$, and because the cost J is convex in $\boldsymbol{u}$, the optimal control sequence $\boldsymbol{u}^*$ for the unconstrained problem over the planning horizon N is given by $\boldsymbol{u} = \boldsymbol{u}^*$ such that $\partial J/\partial \boldsymbol{u}^* = \boldsymbol{0}$.

IV. Reference Signal Prediction

In each receding horizon (RH) window an extrapolation of the reference signal needs to be performed. A two-stage extrapolation scheme is investigated, where each stage is based on a polynomial extrapolation of the reference signal of the form

$$r_n = a_0 + a_1 n + a_2 n^2 + \cdots + a_p n^p, \qquad n = 1, 2, \ldots, N \quad (13)$$

In the first stage, a pth-order polynomial extrapolation of the pilot supplied reference signal is performed. The present and p past values of the pilot supplied reference are used to predict what is actually desired of the system over the planning horizon. This is necessary to determine the right (future) anchor point for the second-stage interpolation. The first-stage extrapolation involves the solution of a set of $p + 1$ linear equations. The second stage then involves the determination of the feasible reference sequence, $\boldsymbol{r}'$, which can be tracked without violating the control constraints. Stage two is similar to stage one, except that it is desired to express this sequence in terms of the known, previously applied values of the reference signal, the aforementioned right anchor point, and an adjustable reference signal at time $n = 1, r_1'$. This second interpolation is accomplished using a p'th-order polynomial fit. To completely determine the polynomial coefficients, $p' + 1$ boundary conditions are required. However, because the proposed control strategy requires expressing the extrapolated reference sequence in terms of r_1', only p' additional conditions must be explicitly known. These boundary conditions consist of $p' - 1$ previously applied values of the reference signal and $\hat{r}_N$, the right anchor point. This two-stage reference extrapolation concept is illustrated in Fig. 2, where a three-points-based second-order ($p = p' = 2$), parabolic, extrapolation is used in both stages. The extrapolation is performed at time k.

At the conclusion of the second-stage extrapolation, $\boldsymbol{r}'$ is linear in r_1' and, thus, the feasible reference sequence can be written in the linear form

$$\boldsymbol{r}' = [r_n'] = \begin{bmatrix} r_1' \\ r_2' \\ r_3' \\ r_N' \end{bmatrix} = \begin{bmatrix} 1 \\ k_2 \\ k_3 \\ k_N \end{bmatrix} r_1' + \begin{bmatrix} 0 \\ h_2 \\ h_3 \\ h_N \end{bmatrix} = \boldsymbol{k} r_1' + \boldsymbol{h} \quad (14)$$

where the k_n are constants determined by the order p of the polynomial extrapolation and the h_n depend only on the present and p past values of the pilot commanded reference signal and the p' previously determined feasible reference values corresponding to the p' previous pilot commanded reference values, which are known at time now. In addition, the coefficients h_n are linear in these past and present reference values. Thus, $\boldsymbol{h}$ is also constant within a given window. Hence, during the current window, and as it relates to the required optimization, $\boldsymbol{r}'$ is explicitly known as a linear function of the as of yet to be obtained r_1'.

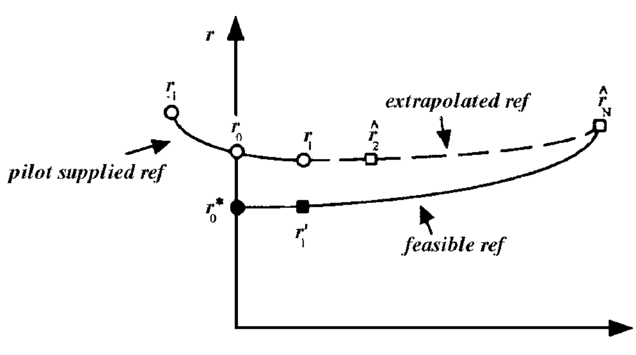

Fig. 2 Second-order two-stage extrapolation.

V. Unconstrained Optimal Control

Given the discrete time system of Eqs. (4–6), the unconstrained LQT solution is based on optimal tracking of the extrapolated reference sequence $\hat{\boldsymbol{r}} = (r_1, \hat{r}_2, \ldots, \hat{r}_N)^T$ within each RH window. The finite-horizon LQ cost function of Eq. (8) is considered for the optimality criterion. Thus, the inputs to the optimization in each window are the current state $\boldsymbol{x}_k$ (referred to as $\boldsymbol{x}_0$ within the window) and the prespecified (extrapolated) reference signal $\hat{\boldsymbol{r}}$, currently referred to as $\boldsymbol{r}$, which are used to determine the unconstrained optimal control sequence $\boldsymbol{u}^*(\boldsymbol{r}; \boldsymbol{x}_0)$. In each window, $\boldsymbol{r}$ is parametrized by r_1.

Direct substitution of the explicit solution of the difference Eq. (15) into the quadratic functional (7) and setting the result equal to zero yields the closed-form optimal control sequence

$$\begin{aligned} \boldsymbol{u}^*(\boldsymbol{r}; \boldsymbol{x}_0) &= \Lambda \boldsymbol{r} + \Pi \boldsymbol{x}_0 + O d \\ &= \Lambda(\boldsymbol{k} r_1 + \boldsymbol{h}) + \Pi \boldsymbol{x}_0 + O d \\ &= \Lambda \boldsymbol{k} r_1 + \Lambda \boldsymbol{h} + \Pi \boldsymbol{x}_0 + O d \end{aligned} \quad (15)$$

where the coefficient matrices $\Lambda \in \boldsymbol{R}^{N \times N}$, $\Pi \in \boldsymbol{R}^{N \times n}$, and $O \in \boldsymbol{R}^N$ depend only on the system parameters ($\boldsymbol{A}$, $\boldsymbol{b}$, $\boldsymbol{c}$, $\boldsymbol{\Gamma}_1$, and $\boldsymbol{\Gamma}_2$) and the LQ weights Q_P, Q_I, and R. Explicit formulas for the Λ, Π, and O coefficient matrices can be found in Ref. 16. An important observation is that $\boldsymbol{u}^*$ is linear in both $\boldsymbol{r}$ and the initial state $\boldsymbol{x}_0 \equiv \boldsymbol{x}_k$. Hence, the unconstrained LQT optimal control solution is specified linearly in terms of the known plant parameters in the coefficient matrices Λ, Π, and O; known past values and the present value of the reference sequence in $\boldsymbol{h}$ and r_1; the current plant state $\boldsymbol{x}_0'$, and the known and constant disturbance d. Obviously, in the unconstrained case, the second-stage extrapolation of the reference signal is redundant.

VI. Control Constraints

The optimal tracking control sequence as determined in the preceding development may violate the actuator constraints. Thus, to avoid the detrimental effects of hard saturation, it may become necessary to modify the exogenous command input to the system and determine a feasible reference sequence $\boldsymbol{r}'$, which can be tracked in a given window within the bounds of the actuator constraints. Because the actual system control $u_k = u_0$ is the only element of $\boldsymbol{u}$ that will actually be applied to the system, only saturations at time $k + 1$ directly attributable to $u_k = u_0$ will be accounted for. Now, $u_k^* = u_k^*(\boldsymbol{r}; \boldsymbol{x}_k)$ and, thus, the question arises: If the input u_k will induce either a rate or amplitude saturation, what is the best reference $\boldsymbol{r}'$ that can be optimally tracked such that the control $u_k' = u_k^*(\boldsymbol{r}'; \boldsymbol{x}_k)$ will not induce an actuator saturation at time $k + 1$? Best here refers to closeness to the pilot input reference signal. Because the extrapolation is done such that the reference $\boldsymbol{r}' = \boldsymbol{k} r_1 + \boldsymbol{h}$, where the $\boldsymbol{k}$ and $\boldsymbol{h}$ vectors are effectively constants within each RH window, the preceding question is tantamount to determining a feasible r_1'. Thus, $u_0 \equiv u_k$ can be written in the form

$$\begin{aligned} u_k = {} & \boldsymbol{k}_x \boldsymbol{x}_k + \boldsymbol{k}_r [r_{k+1-p}, \ldots, r_{k+1}]^T \\ & + \boldsymbol{k}_{r^*}\left[r^*_{k+2-p'}, \ldots, r^*_k\right]^T + k_{r'} r'_{k+1} + k_d d \end{aligned} \quad (16)$$

where $\boldsymbol{k}_x = \Pi(1, :)$ (the first row of Π), $k_{r'} = [\Lambda \boldsymbol{k}](1)$ (the first element of the vector $\Lambda \boldsymbol{k}$), $k_d = O(1)$, and k_r and k_{r^*} result from algebraic manipulations on $\Lambda \boldsymbol{h}$. For example, in the case $p = p' = 2$,

$$\boldsymbol{k}_r = \left[\frac{1}{2}\sum_{m=1}^{N} (m^2 - m)\Lambda(1, m)\right]\left[1 - 2\left(1 + \frac{1}{N}\right)\frac{N+1}{N-1}\right] \quad (17)$$

$$k_{r^*} = \sum_{m=1}^{N} \left\{\left[1 - \left(1 + \frac{1}{N}\right)m + \frac{1}{N}m^2\right]\Lambda(1, m)\right\} \quad (18)$$

Now, $\delta_{k+1} = \boldsymbol{c}_\delta \boldsymbol{x}_{\delta_{k+1}} = \boldsymbol{c}_\delta(\boldsymbol{A}_\delta \boldsymbol{x}_{\delta_k} + \boldsymbol{b}_\delta \delta_{c_k})$, where $\delta^*_{c_k} \equiv u^*_k \equiv u^*_0$ from the preceding development. Thus, the actuator displacement constraints of Eq. (2) applied at time k can be transformed into explicit constraints on r'_1 given by

$$f_d \le r'_1 \le g_d \tag{19}$$

where the numbers

$$f_d = \frac{\delta_{\min} - \boldsymbol{c}_a[\boldsymbol{A} + \boldsymbol{b}\boldsymbol{k}_x]\boldsymbol{x}_k}{\boldsymbol{c}_a\boldsymbol{b}k_{r'}} - \frac{\boldsymbol{c}_a\boldsymbol{b}\boldsymbol{k}_r[r_{k+1-p}, \ldots, r_{k+1}]^T}{\boldsymbol{c}_a\boldsymbol{b}k_{r'}} - \frac{\boldsymbol{c}_a\boldsymbol{b}\left(\boldsymbol{k}_{r^*}\left[r^*_{k+2-p'}, \ldots, r^*_{k-1}\right] + \boldsymbol{k}_d d\right)}{\boldsymbol{c}_a\boldsymbol{b}k_{r'}} \tag{20}$$

$$g_d = \frac{\delta_{\max} - \boldsymbol{c}_a[\boldsymbol{A} + \boldsymbol{b}\boldsymbol{k}_x]\boldsymbol{x}_k}{\boldsymbol{c}_a\boldsymbol{b}k_{r'}} - \frac{\boldsymbol{c}_a\boldsymbol{b}\boldsymbol{k}_r[r_{k+1-p}, \ldots, r_{k+1}]^T}{\boldsymbol{c}_a\boldsymbol{b}k_{r'}} - \frac{\boldsymbol{c}_a\boldsymbol{b}\left(\boldsymbol{k}_{r^*}\left[r^*_{k+2-p'}, \ldots, r^*_{k-1}\right] + \boldsymbol{k}_d d\right)}{\boldsymbol{c}_a\boldsymbol{b}k_{r'}} \tag{21}$$

and $\boldsymbol{c}_a = [\boldsymbol{0} \mid \boldsymbol{c}_\delta \mid 0]$. In the event that $\boldsymbol{c}_a\boldsymbol{b}k_{r'} < 0$, the inequality signs of Eq. (19) are reversed.

Similarly, the rate constraints of Eq. (3) applied at time k are

$$f_r \le r'_1 \le g_r \tag{22}$$

where the numbers

$$f_r = \frac{\Delta\,\delta_{\min} - \boldsymbol{c}_a[(\boldsymbol{A} - \boldsymbol{I}) + \boldsymbol{b}\boldsymbol{k}_x]\boldsymbol{x}_k}{\boldsymbol{c}_a\boldsymbol{b}k_{r'}} - \frac{\boldsymbol{c}_a\boldsymbol{b}\boldsymbol{k}_r[r_{k+1-p}, \ldots, r_{k+1}]^T}{\boldsymbol{c}_a\boldsymbol{b}k_{r'}} + \frac{\boldsymbol{c}_a\boldsymbol{b}\boldsymbol{k}_{r^*}\left[r^*_{k+2-p'}, \ldots, r^*_{k-1}\right] + \boldsymbol{c}_a\boldsymbol{b}\boldsymbol{k}_d d}{\boldsymbol{c}_a\boldsymbol{b}k_{r'}} \tag{23}$$

$$g_r = \frac{\Delta\,\delta_{\max} - \boldsymbol{c}_a[(\boldsymbol{A} - \boldsymbol{I}) + \boldsymbol{b}\boldsymbol{k}_x]\boldsymbol{x}_k}{\boldsymbol{c}_a\boldsymbol{b}k_{r'}} - \frac{\boldsymbol{c}_a\boldsymbol{b}\boldsymbol{k}_r[r_{k+1-p}, \ldots, r_{k+1}]^T}{\boldsymbol{c}_a\boldsymbol{b}k_{r'}} + \frac{\boldsymbol{c}_a\boldsymbol{b}\boldsymbol{k}_{r^*}\left[r^*_{k+2-p'}, \ldots, r^*_{k-1}\right] + \boldsymbol{c}_a\boldsymbol{b}\boldsymbol{k}_d d}{\boldsymbol{c}_a\boldsymbol{b}k_{r'}} \tag{24}$$

and in the event that $\boldsymbol{c}_a\boldsymbol{b}k_{r'} < 0$, the inequality signs of Eq. (22) are reversed.

The most strict inequalities are used to determine $r_{\min}$ and $r_{\max}$ such that Eqs. (19) and (22) are both satisfied when $r_{\min} \le r' \le r_{\max}$. Here, $r_{\min} = \max(f_d, f_r)$ and $r_{\max} = \min(g_d, g_r)$ for $\boldsymbol{c}_a\boldsymbol{b}k_{r'} > 0$ or $r_{\min} = \max(g_d, g_r)$ and $r_{\max} = \min(f_d, f_r)$ for $\boldsymbol{c}_a\boldsymbol{b}k_{r'} < 0$, and r'_1 is chosen accordingly, viz.,

$$r'_1 = \begin{cases} r_{\min}, & \text{for} \quad r_1 < r_{\min} \\ r_1, & \text{for} \quad r_{\min} \le r_1 \le r_{\max} \\ r_{\max}, & \text{for} \quad r_1 > r_{\max} \end{cases} \tag{25}$$

The value of r'_1 given by Eq. (25) is inserted into Eq. (16), thus obtaining the optimal control signal.

When the hard control constraints are active, the end result is tantamount to a nonlinear scaling of $r_1 = r_{k+1}$, yielding a feasible reference $r'_1 = r'_{k+1}$. Hence, the state feedback structure is unaffected and bounded-input bounded-output (BIBO) stability of the closed-loop system (from r' to y) is maintained. That is, within each optimization window, the linear LQ optimal control is determined for tracking $\boldsymbol{r}'$, a feasible reference that will not cause saturations to occur. Furthermore, during small signal operation, $r'_{k+1} = r_{k+1}$, and the linear performance characteristics are preserved: Small signal performance is not sacrificed to accommodate the actuator constraints.

A crucial observation is that $|r'_{k+1}| \le |r_{k+1}|$ does not necessarily hold. The case $|r'_{k+1}| > |r_{k+1}|$ is, indeed, possible, and, e.g., it is also possible that $r_{k+1} = 0$ whereas $r'_{k+1} \ne 0$. Hence, a rather general adjustment of the exogenous reference signal is employed in order to address the manual tracking problem with both amplitude and rate control constraints.

VII. Flight Control Example

The aircraft plant used here represents the short-period dynamics of an F-16 derivative, at the flight condition 10,000 ft, Mach 0.7. Specifically, the bare plant's state-space model is given by

$$\begin{bmatrix} \dot{\alpha} \\ \dot{q} \end{bmatrix} = \begin{bmatrix} Z_\alpha & Z_q \\ M_\alpha & M_q \end{bmatrix} \begin{bmatrix} \alpha \\ q \end{bmatrix} + \begin{bmatrix} Z_\delta \\ M_\delta \end{bmatrix} \delta \tag{26}$$

where the units of angle of attack α and pitch rate q are radians and radians per second, respectively, with $Z_\alpha = -1.15$, $Z_q = 0.9937$, $Z_\delta = -0.177$, $M_\alpha = 3.724$, $M_q = -1.26$, and $M_\delta = -19.5$. Additionally, a first-order actuator with bandwidth of 20 rad/s is used, with amplitude and rate constraints of 0.37 rad and 1 rad/s, respectively. The augmented discrete-time linear model, including the actuator state and an integral control state, and using a sampling interval of $T = 0.01$ s, is given by

$$\begin{bmatrix} \alpha_{k+1} \\ q_{k+1} \\ \delta_{k+1} \\ z_{k+1} \end{bmatrix} = \begin{bmatrix} 0.9887 & 0.0098 & -0.0025 & 0 \\ 0.0368 & 0.9877 & -0.1756 & 0 \\ 0 & 0 & 0.8187 & 0 \\ -0.000368 & -0.009877 & 0.001938 & 1 \end{bmatrix} \times \begin{bmatrix} \alpha_k \\ q_k \\ \delta_k \\ z_k \end{bmatrix} + \begin{bmatrix} 0 \\ 0 \\ 0.1813 \\ 0 \end{bmatrix} \delta_{c_k} + \begin{bmatrix} 0 \\ 0 \\ 0 \\ 0.01 \end{bmatrix} r_k \tag{27}$$

Pitch rate q is the output of interest, and thus the output row vector $\boldsymbol{c} = [0 \;\; 1 \;\; 0 \;\; 0]$.

In terms of the reference signal prediction, $p = p' = 2$ has fared well in simulation studies, without any appreciable gain in performance by using higher-order extrapolations. The physical prediction horizon of the extrapolation is given by TN, which is in this case $0.01N$ s. The tracking characteristics of the closed-loop system depend on the weights Q_I, Q_P, R, and N. Increasing Q_I, Q_P, or N, or decreasing R translates to a higher gain controller and, thus, tighter tracking. Thus, in terms of the tracking performance, virtually any desired characteristics can be obtained with virtually any value of N, by appropriately adjusting the weights. Of course, higher gain controllers increase the likelihood of infringement of the actuator constraints, but the LQT controller mitigates these effects. $N > 1$ is required for the extrapolational algorithm to be applicable, i.e., for $N = 1$, $\hat{\boldsymbol{r}} = [r_1]$, which is known and no extrapolation is then required.

In the simulations, $p = p' = 2$, viz., parabolic extrapolation is used. The resulting LQT control law is, thus, given by

$$u_k = \delta_{c_k} = \boldsymbol{k}_x \boldsymbol{x}_k + \boldsymbol{k}_r[r_{k-1}, r_k, r_{k+1}]^T + k_{r^*} r^*_k + k_{r'} r'_{k+1} \tag{28}$$

where the specific gain values depend only on the horizon N, the plant parameters $\boldsymbol{A}$, $\boldsymbol{b}$, and $\boldsymbol{c}$, and the LQ weights Q_I, Q_P, and R. In Eq. (28), r^*_k is the feasible reference, which was determined at the previous time step. Having linearized about a trim flight condition, the disturbance $d = 0$.

The input signal used for each simulation is a pitch doublet prefiltered by $F(s)$, the flying qualities/reference model's dynamics,

$$F(s) = \frac{19.5s + 23}{s^2 + 7s + 16.25} \tag{29}$$

The prefilter attenuates the broadband dynamics introduced by the human operator (the pilot), which closes an additional outer loop about the flight control system.

The proposed LQT tracker is compared to a straightforward infinite horizon linear quadratic regulator (LQR)-based tracker commonly used, e.g., see Ref. 6, a simplification where a plant input signal of $u_k = r_{k+1} - \boldsymbol{k}_{\mathrm{LQR}}\boldsymbol{x}_k$ is used and where $\boldsymbol{k}_{\mathrm{LQR}}$ is the infinite horizon LQR control law gain; regulator-based trackers of this type may require special consideration in the selection of the LQ weights to ensure that a steady-state gain of 1 is achieved. The inclusion of the integral control state ensures that the regulator-based tracker will have unity dc gain. In general, however, integral control is not required for tracking when state feedback is used and the

LQT paradigm is employed; rather, it is needed to address model uncertainty and unmodeled disturbance rejection.

The simulation results in Fig. 3 demonstrate that the proposed optimization-based, RHPC formulation and the use of the extrapolated reference signal does improve the tracking performance. In this example, the weights $Q_I = 47.0$, $Q_P = 0.29$, and $R = 0.91$ are chosen to obtain the desired closed-loop performance. Now, as N becomes large, the state feedback gain vector approaches the (infinite-horizon) LQR solution provided gain. For the example at hand, it transpires that, for $N = 60$, there is no appreciable difference between $\boldsymbol{k}_x$ and the infinite horizon LQR gain $\boldsymbol{k}_{\mathrm{LQR}}$ and, thus, there is nothing to be gained by selecting $N > 60$. (Note that this value depends not only on the plant parameters but also on the LQ weights.) Thus, for a fair comparison, the LQT optimization and prediction horizon $N = 60$ is selected (physically, the reference signal is predicted 0.6 s into the future), and the actuator constraints are not enforced. The benefit of the LQT approach, viz., tighter tracking, is evident from Fig. 3. The closed-loop frequency responses resulting from these two control strategies are compared in Fig. 4, which shows that the beneficial effect of including the reference signal in the optimization is to increase the bandwidth and minimize the phase lag of the closed-loop system.

The next simulation demonstrates the detrimental effects of actuator saturations when they are not accounted for in the design process. Again, the regulator-based tracker of the earlier example is considered, and the results are compared to the performance of the LQT controller. In this case, the planning horizon $N = 5$ is used in the LQT controller, and to greatly exacerbate the actuator saturation problem, a very high-gain controller is considered, and it is attempted to track a high-amplitude reference signal. Specifically, to obtain high-gain action, the LQ weights are modified from the earlier example as follows. Q_P is increased by a factor of 32, and Q_I is increased by a factor of 60. Furthermore, the amplitude of the reference signal is tripled.

First, the unconstrained response is shown in Fig. 5, where it is noted that the LQT controller achieves tighter tracking. The constrained response is shown in Figs. 6 and 7. As expected, the LQT response is somewhat degraded; the constrained system simply cannot perfectly track this reference signal. The response, nevertheless, is relatively well behaved. Furthermore, note that the apparent hard saturations in rate are, in fact, imposed by the controller. Thus, the feasible references include those that result in the actuator riding the limit, but not those that would exceed those constraints. The heuristic LQR-based tracker (which did not account for the actuator constraints in the design process) on the other hand, yields totally unacceptable performance. Thus, it is demonstrated that the proposed LQT strategy can deliver tight (high-gain) dynamic tracking performance, while at the same time mitigate the impact of hard actuator constraints during high-amplitude maneuvers.

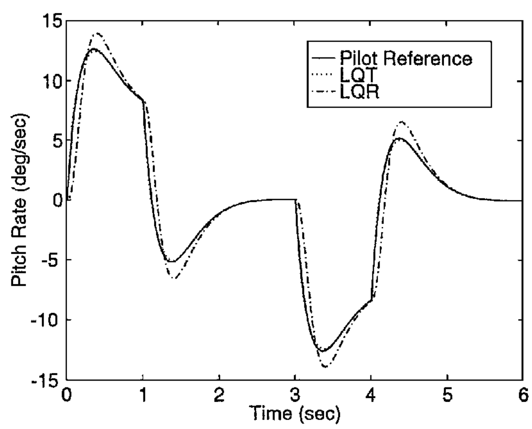

Fig. 3 LQT, N = 60 vs LQR unconstrained, linear case.

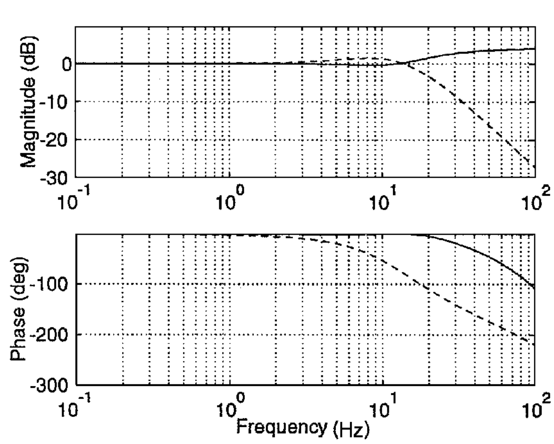

Fig. 4 Closed-loop frequency response, LQT (—) vs LQR.

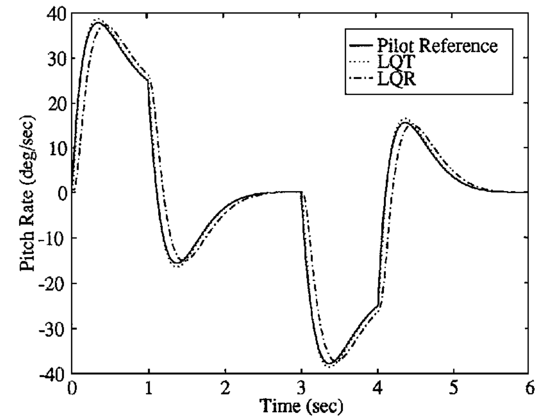

Fig. 5 High-gain, high-amplitude tracking, unconstrained.

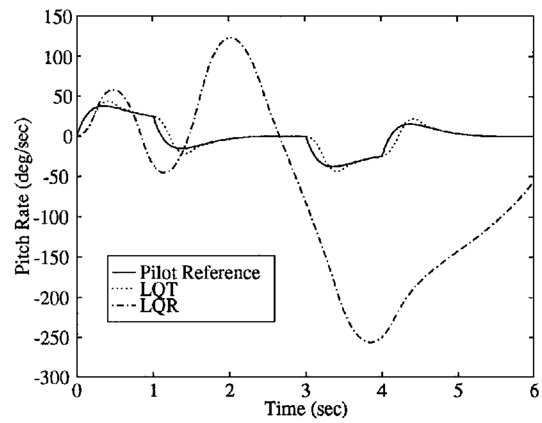

Fig. 6 High-gain, high-amplitude tracking, constrained.

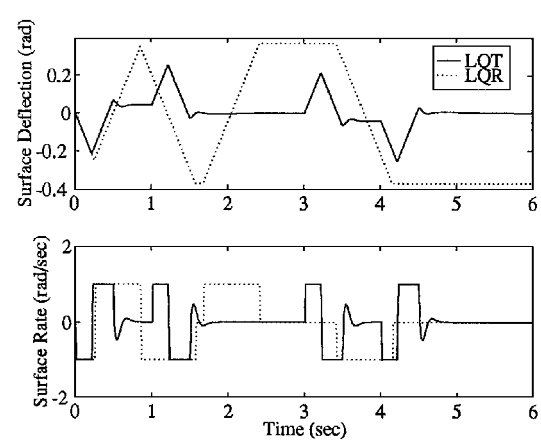

Fig. 7 Control surface response.

VIII. Discussion

The approach presented here yields a computationally inexpensive, closed-form and real-time implementable solution to the constrained tracking problem. Specifically, the solution is given by an explicit control law of the form of Eq. (16), where the gains $\boldsymbol{k}_x$, $\boldsymbol{k}_r$, $\boldsymbol{k}_{r^*}$, $\boldsymbol{x}_{r'}$, and k_d are constants, which depend only on the horizon N, the plant parameters $\boldsymbol{A}$, $\boldsymbol{b}$, $\boldsymbol{c}$, $\boldsymbol{\Gamma}_1$, and $\boldsymbol{\Gamma}_2$, and the LQ weights Q_I, Q_P, and R, and, therefore, can be computed off-line. Note that $\boldsymbol{x}_k$ is the current state, $\boldsymbol{r}_j$ are the pilot's commands, r'_{k+1} is the (yet to be determined) current feasible reference, the r^*_j are the previous feasible (and, therefore, applied to the control system and known) reference signals, and d is the known constant disturbance. Thus, the constrained LQT solution is expressed as a fixed gain controller, which operates on the current values of the state, reference input, and feasible reference, p previous values of the pilot desired reference and $p' - 1$ previous values of the (actually input) feasible reference. Note, however, that this control is only linear in appearance, for in the case of large inputs or strong deviations from trim, the feasible reference signal r'_{k+1} is nonlinearly determined.

When actuator saturation is not exercised, as in small signal operation, the signals r^* and r' are simply the pilot input r, and full linear action is realized. Thus, when the actuator saturation limits are not infringed, the control u_k is linear in $\boldsymbol{x}_k, r_{k+1-p}, \ldots, r_{k+1}$, and d, and Eq. (16) can be written

$$u_k = \boldsymbol{k}_x \boldsymbol{x}_k + \boldsymbol{k}_R [r_{k+1-p}, \ldots, r_{k+1}]^T + k_d d \qquad (30)$$

with

$$\boldsymbol{k}_R = \boldsymbol{k}_r + [0 \ | \ \boldsymbol{k}_{r^*} \ | \ k_{r'}] \qquad (31)$$

The inclusion of the reference signal's past values introduces additional dynamics and causes an augmentation of the closed-loop system, yielding p additional states. In the linear case, however, the only effect on the closed-loop system lies in the number and placement of the closed-loop zeros, as the additional p poles will always be at $s = -\infty$.

In the constrained case, the control law is nonlinear due to the nonlinear calculation of $\boldsymbol{u}$ in Eq. (16), which is repeated here:

$$u_k = \boldsymbol{k}_x \boldsymbol{x}_k + \boldsymbol{k}_r [r_{k+1-p}, \ldots, r_{k+1}]^T + \boldsymbol{k}_{r^*} \left[r^*_{k+2-p'}, \ldots, r^*_k\right]^T$$
$$+ k_d d + k_{r'} f\left(\boldsymbol{x}_k, r_{k+1-p}, \ldots, r_{k+1}, r^*_{k+2-p'}, \ldots, r^*_k, d\right)$$

However, the function f is piecewise linear in its listed arguments. The dependence of the nonlinear component f not only on previous (closed-loop system) input values but also on previous state values (via the $r^*_{k+2-p'}, \ldots, r^*_k$) augments the system, for $r^*_{k+1} = f_{r^*}(\boldsymbol{x}_k, r_{k+1-p}, \ldots, r_{k+1}, r^*_{k+2-p'}, \ldots, r^*_k, d)$, and will clearly affect the closed-loop poles.

IX. Conclusions

The proposed optimization-based approach to tracking includes actuator dynamics and accounts for both rate and displacement actuator (not control) constraints, addresses the dynamic and transient nature of the manual tracking problem, has no inherent requirement for stability of the open-loop plant, and employs full state feedback. Furthermore, the resulting piecewise linear control law is computationally inexpensive, does not require the use of on-line numerical search/optimization routines, is easily implementable in real time, and small signal performance is maintained. At the same time, good responses to large exogenous (pilot) commands are obtained.

Finally, in the context of manual flight control, an additional benefit of the proposed tracking control paradigm is in the handling qualities arena, for the proposed saturation mitigating controller eliminates the compensator windup problem and will, therefore, tend to delay or preclude the onset of nonlinear, viz., actuator saturation caused, pilot-induced oscillations.

The following limitation of the controller is noted. BIBO stability from r to y is not guaranteed; in other words, there may exist reference signals from the pilot that, due to the actuator constraints, will result in unbounded r', poor tracking, and the controlled variable will not be bounded, resulting in a departure that the proposed control system for saturation mitigation cannot preclude. To guarantee BIBO stability, constraints above and beyond saturation bounds must be enforced, viz., the state vector should evolve in a compact subset of the state space and, therefore, additional invariance arguments must be employed. In current practice, a prefilter and a limiter are placed at the pilot's stick output to keep this problem from occurring.

References

[1]Bernstein, D. S., "Optimal Nonlinear, but Continuous, Feedback Control of Systems with Saturating Actuators," *Proceedings of the 32nd Conference on Decision and Control*, IEEE Control Systems Society, Omnipress, Madison, WI, 1993, pp. 2533–2537.

[2]Blackwell, C. C., "Actuator Saturation and Control System Performance," *Proceedings of the 1993 American Control Conference*, Vol. 3, IEEE Control Systems Society, Omnipress, Madison, WI, 1993, pp. 2420, 2421.

[3]Campo, P. J., and Morari, M., "Robust Control of Processes Subject to Saturation Nonlinearities," *Computers in Chem Engineering*, Vol. 14, Nos. 4/5, 1990, pp. 343–358,

[4]Pachter, M., and Miller, R. B., "Manual Flight Control with Saturating Actuators," *IEEE Control Systems Magazine* (to be published).

[5]Chandler, P. R., Mears, M. J., and Pachter, M., "A Hybrid LQR/LP Approach for Addressing Actuator Saturation in Feedback Control," *1994 Conference on Decision and Control* (Orlando, FL), IEEE Control Systems Society, Omnipress, Madison, WI, 1994, pp. 3860–3867.

[6]D'Azzo, J. J., and Houpis, C. H., *Linear Control System Analysis & Design*, McGraw–Hill, New York, 1988.

[7]Gilbert, E. G., Kolmanovsky, I., and Tan, K. T., "Nonlinear Control of Discrete-Time Linear Systems with State and Control Constraints: A Reference Governor with Global Convergence Properties," *Proceedings of the 33rd Conference on Decision and Control*, IEEE Control Systems Society, Omnipress, Madison, WI, 1994, pp. 144–149.

[8]Gilbert, E. G., and Tan, K. T., "Linear Systems with State and Control Constraints: The Theory and Application of Maximal Output Admissible Sets," *IEEE Transactions on Automatic Control*, Vol. AC-36, No. 9, 1991, pp. 1008–1020.

[9]Gyugyi, P. J., and Franklin, G., "Multivariable Integral Control with Input Constraints," *Proceedings of the 32nd IEEE Conference on Decision and Control*, Vol. 3, IEEE Control Systems Society, Omnipress, Madison, WI, 1993, pp. 2505–2510.

[10]Hanus, R., Kinnaert, M., and Henrotte, J. L., "Conditioning Technique, a General Antiwindup and Bumpless Transfer Method," *Automatica*, Vol. 23, 1987, pp. 729–739.

[11]Hess, R. A., and Snell, S. A., "Flight Control Design with Actuator Saturation: SISO Systems with Unstable Plants," AIAA Paper 95-0336, Jan. 1995.

[12]Hess, R. A., and Snell, S. A., "Feedback Design for Unstable Plants with Saturating Nonlinearities; Single-Input, Single-Output," *Journal of Guidance, Control, and Dynamics*, Vol. 19, No. 1, 1996, pp. 191–197; Errata, Vol. 19, No. 6, 1996, p. 1200.

[13]Horowitz, I., "Feedback Systems with Rate and Amplitude Limiting," *International Journal of Control*, Vol. 409, No. 6, 1984, pp. 1215–1229.

[14]Kapasouris, P., and Athans, M., "Control Systems with Rate and Magnitude Saturation for Neutrally Stable Open-Loop Systems," *Proceedings of the 29th Conference on Decision and Control*, Vol. 6, IEEE Control Systems Society, Omnipress, Madison, WI, 1990, pp. 3404–3409.

[15]Kapasouris, P., Athans, M., and Stein, G., "Design of Feedback Control Systems for Stable Plants with Saturating Actuators," *Proceedings of the 27th Conference on Decision and Control* (Austin, TX), IEEE Control Systems Society, Omnipress, Madison, WI, 1988, pp. 469–479.

[16]Miller, R. B., "A New Approach to Manual Tracking Flight Control with Amplitude and Rate Constrained Dynamic Actuators," Ph.D. Dissertation, Dept. of Electrical Engineering, U.S. Air Force Inst. of Technology, Wright–Patterson AFB, OH, March 1997.

[17]Pachter, M., Chandler, P. R., and Mears, M., "Control Reconfiguration with Actuator Rate Saturation," *Proceedings of the American Control Conference* (Seattle, WA), IEEE Control Systems Society, Omnipress, Madison, WI, 1995, pp. 3495–3499.

[18]Pachter, M., Chandler, P. R., and Mears, M., "Reconfigurable Tracking Control with Saturation," *Journal of Guidance, Control, and Dynamics*, Vol. 18, No. 5, 1995, pp. 1016–1022.

[19]Popov, V. M., *Hyperstability of Control Systems*, Springer, Berlin, 1974.

[20]Powers, B. G., "Space Shuttle Longitudinal Landing Flying Qualities," *Journal of Guidance, Control, and Dynamics*, Vol. 9, No. 5, 1986, pp. 566–572.

[21]Rodriguez, A. A., and Wang, Y., "Saturation Prevention Strategies for an Unstable Bank-To-Turn (BTT) Missile: Full Information," Dept. of EE, Arizona State Univ., Tempe, AZ, 1995.

[22]Tsirukis, A. G., and Morari, M., "Controller Design with Actuator Constraints," *Proceedings of the Conference on Decision and Control*, IEEE Control Systems Society, Omnipress, Madison, WI, 1992, pp. 2623–2628.